Current Biology, Volume *30*

Supplemental Information

Microtubule-Mediated Wall Anisotropy Contributes to Leaf Blade Flattening

Feng Zhao, Fei Du, Hadrien Oliveri, Lüwen Zhou, Olivier Ali, Wenqian Chen, Shiliang Feng, Qingqing Wang, Shouqin Lü, Mian Long, René Schneider, Arun Sampathkumar, Christophe Godin, Jan Traas, and Yuling Jiao

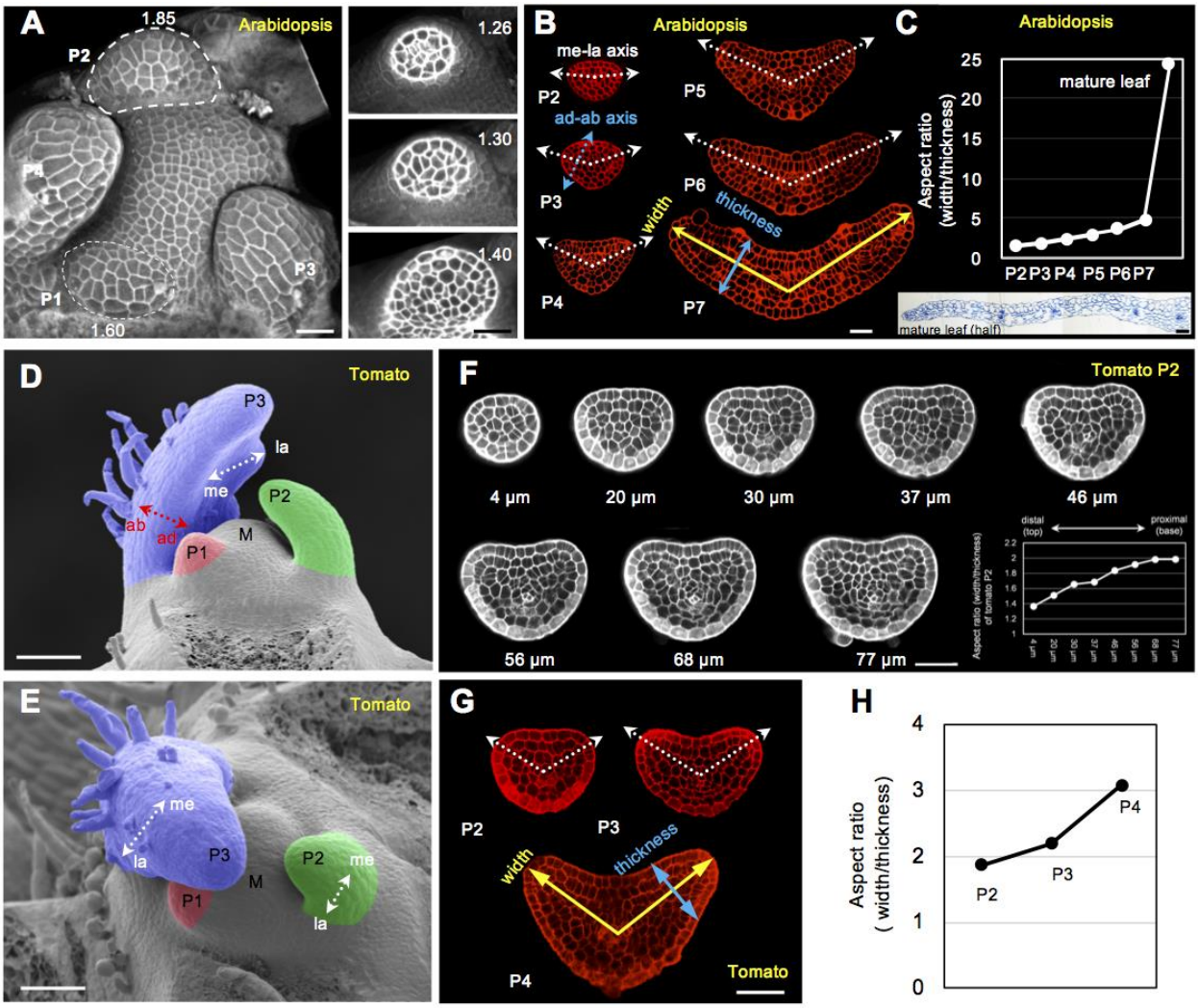

Figure S1. Anisotropic Growth of Arabidopsis and Tomato Leaves, Related to Figure 1

(**A**) Overview of vegetative meristem in Arabidopsis, aspect ratios of contours around the organ basis (left panel) and serial sections through P_2 of the same meristem (right panel) showing a gradient in aspect ratio from bottom (1.85) to top (1.26). (**B**) Cross sections of Arabidopsis leaf primordia (P_2-P_7) and mature leaf (right bottom) showing that the growth of leaf primordia is higher along the medio-lateral axis (me-la axis, white) when compared to the adaxial-abaxial axis (ad-ab axis, blue), which generates a flat form of mature leaves. (**C**) Quantification of width/thickness ratios in Arabidopsis leaves. Leaf width is defined as twice the medio-lateral axis connecting the center to the farthermost points on the outline of a leaf cross-section. (**D** and **E**) Scanning electron micrographs of a tomato shoot apex (**D**, side view; **E**, top view) show that

the leaf primordia initiate surrounding the shoot apical meristem with an anisotropic growth more along the medio-lateral axis (me-la) than along the adaxial-abaxial axis (ad-ab), resulting in an increase in asymmetry (P_2/P_3) shape. P_1 (red), youngest leaf primordium; P_2 (green), second youngest leaf primordium; P_3 (blue), third youngest leaf primordium; M, shoot apical meristem. (**F**) Serial section through tomato P_2 organ to show the gradient of flatness from top to bottom. Measurement performed as indicated in STAR Methods (**G**) Cross sections of tomato leaf primordia (P_2-P_4) showing that the growth of leaf primordia is anisotropic along the medio-lateral axis (white dashed line). (**H**) Quantification of width/thickness ratios in tomato leaves. Leaf width is defined as twice the medio-lateral axis connecting the center to the farthermost points on the outline of a leaf cross-section. Scale bar, 20 μm (**A**, and **B** white); 50 μm in (**B** black, **F** and **G**); 100 μm in (**D** and **E**).

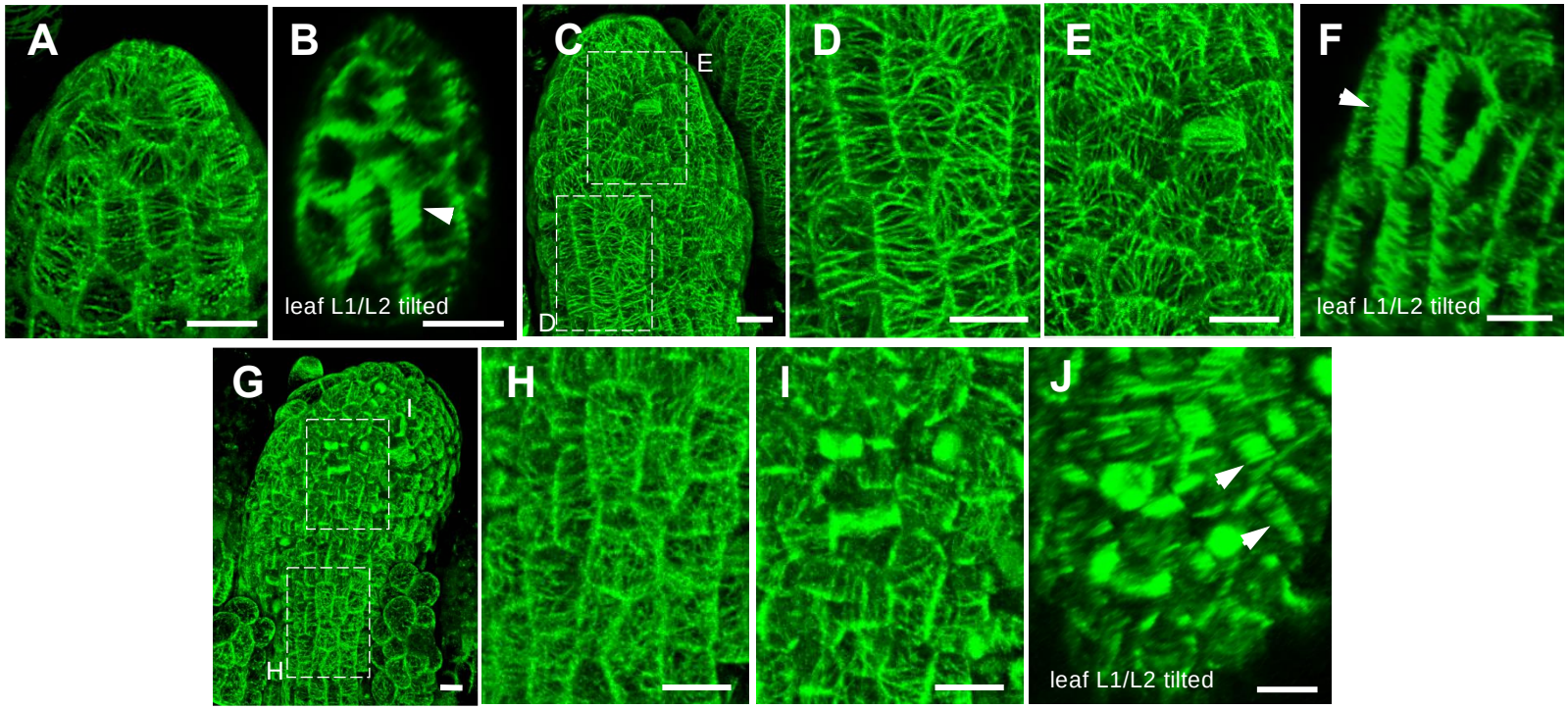

Figure S2. Microtubule Organization in Developing Arabidopsis Leaves, Related to Figure 1

(**A**) Young leaf primordium, at stage around 1 DAI, expressing GFP-MBD, top view, showing anisotropic microtubules. (**B**) Tilted image of (**A**) showing anisotropic microtubule arrays (arrow). (**C** to **F**) Slightly older leaf showing different microtubule arrangements. Boxed areas detailed in (**D**) show cells with anisotropic microtubule arrays, and (**E**) cells with isotropic microtubule arrays. (**F**) Tilted version of (**D**), showing anisotropic microtubules oriented in ad-abaxial direction (arrow). (**G** to **J**) Another example showing isotropic microtubule arrays at leaf surface. (**H** to **I**) Detailed isotropic microtubule arrays in different boxed areas in (**G**). A tilted version of (**I**) is shown in (**J**). Arrows indicated anisotropic microtubule arrays in ad-abaxial walls. Scale bars, 10 μm.

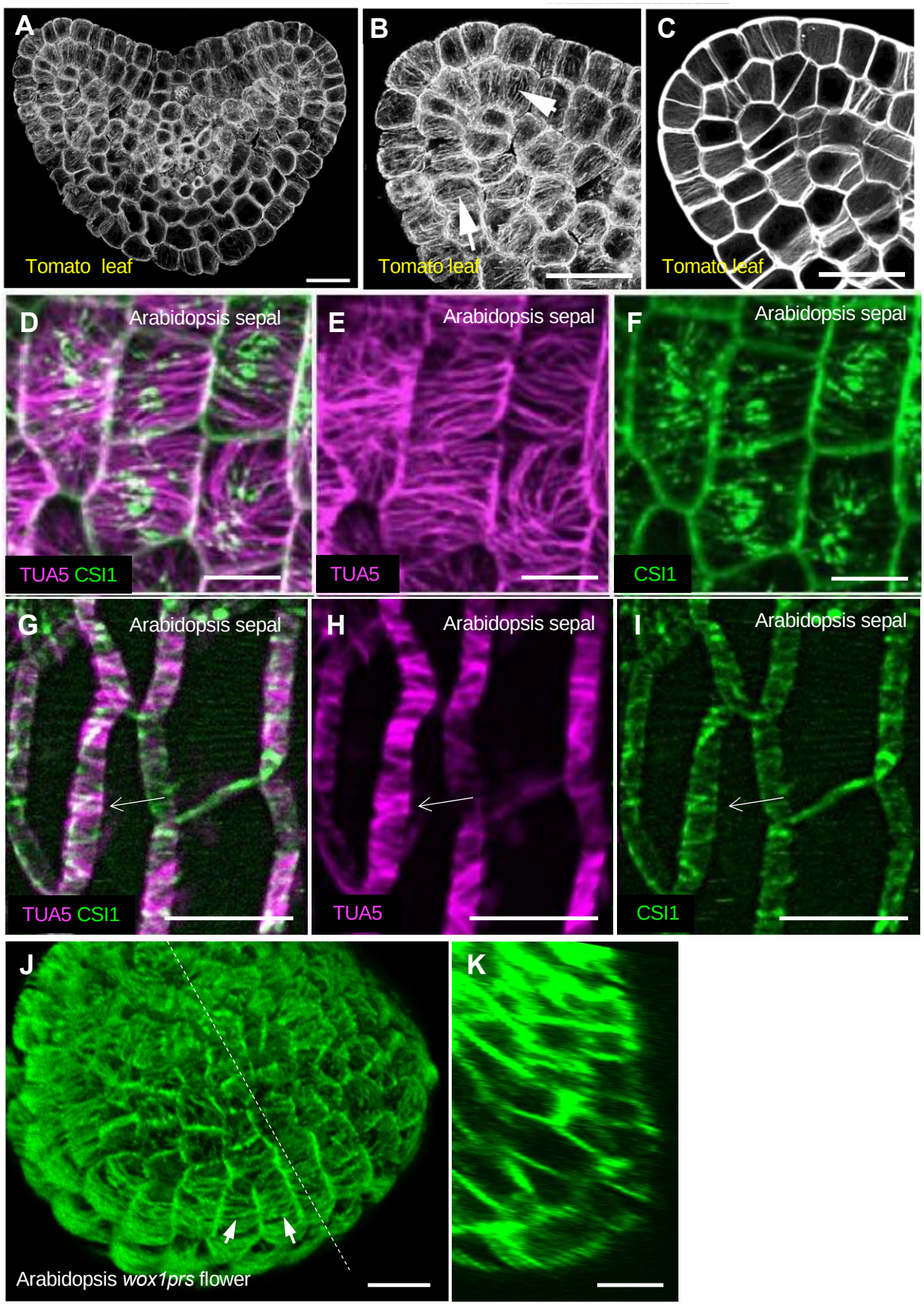
A
Tomato leaf
B
Tomato leaf
C
Tomato leaf
D
Arabidopsis sepal
TUA5 CSI1
E
Arabidopsis sepal
TUA5
F
Arabidopsis sepal
CSI1
G
Arabidopsis sepal
TUA5 CSI1
H
Arabidopsis sepal
TUA5
I
Arabidopsis sepal
CSI1
J
Arabidopsis wox1prs flower
K

Figure S3. Organization of Microtubules and Cellulose Fibers along Adaxial-Abaxial Axis in Tomato and Arabidopsis, Related to Figure 1

(**A** and **B**) The organization of cortical microtubules in the cross section of a tomato P_3 by immunostaining with tubulin antibody. (**A**) overview, (**B**) shows the magnification of a part of (**A**). Arrow heads show ad-abaxial microtubules. (**C**) The orientation of cellulose microfibrils in the cross section of a tomato P_3 stained by Direct Red 23 dye. (**D** to **I**) Live imaging of 3×YFP-labelled Cellulose Synthase Interacting 1 (CSI1/POM2, green) in mCherry-TUA5 (pink) background sepals. (**D** to **F**) average projections to reveal CSI trajectories along microtubules on periclinal surface membrane. (**G** to **I**) show CSI trajectories along ad-abaxial walls. Note anticlinal trajectories of CSI (arrows). Imaging by *z*-stacking (0.3 μm steps) and time-lapsing (1 min intervals) for 15 min. (**J** to **K**) Microtubule organization in Arabidopsis *wox1 prs* sepal primordium. (**J**) Young *wox1 prs* flower bud expressing GFP-MBD showing anisotropic microtubules along the abaxial sepal surface (arrows). (**K**) Section image cutting along the dashed line in (**A**) showing the emergence of young sepal primordium. Scale bars, 20 μm in (**A** to **C**), 10 μm in (**D** to **K**).

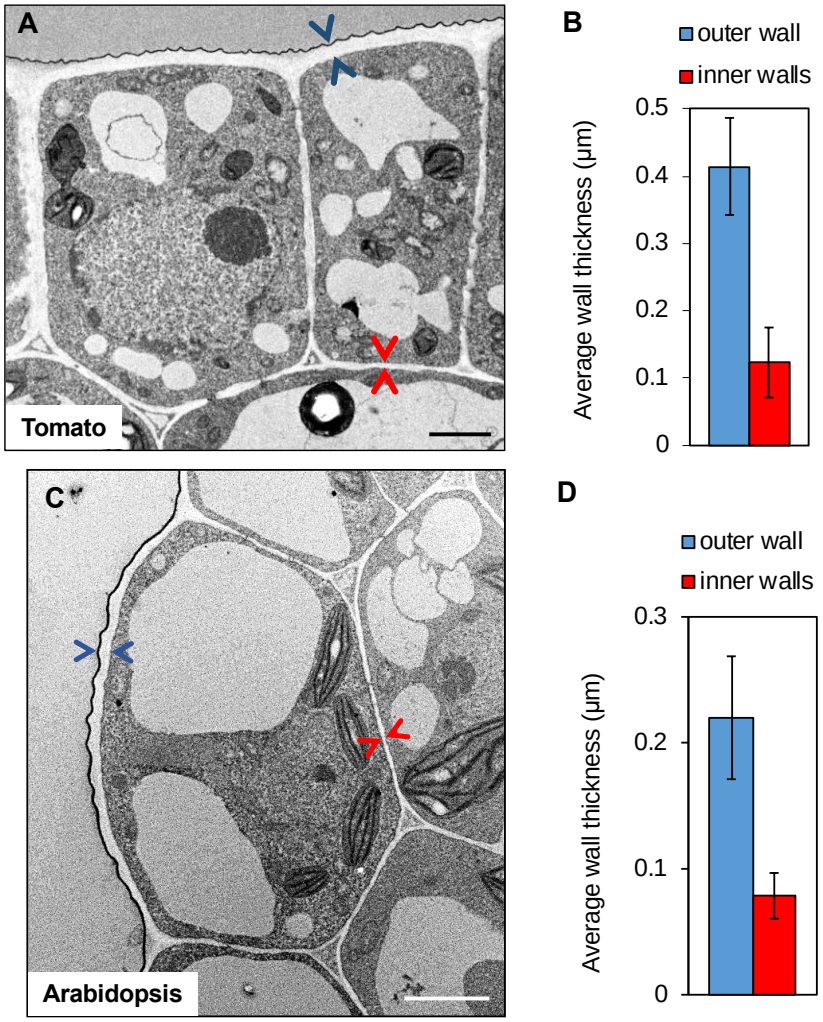

Figure S4. Cell Wall Thickness in Tomato and Arabidopsis Leaf Primordia, Related to Figure 3

(**A**) TEM micrograph of the epidermal cell layer in tomato P_3 leaf primordium cross section showing the outer cell wall (between blue arrowheads) is thicker than inner cell walls (between red arrowheads). (**B**) Quantification of (**A**) showing the outer cell wall is around 3 times as thick as inner cell walls. Cell wall thickness is measured in 159 cells from the cross sections of 3 individual tomato P_3. **(C)** TEM micrograph of the epidermal cell layer in Arabidopsis P_4 leaf primordium cross section showing the outer cell wall (between blue arrowheads) is thicker than inner cell walls (between red arrowheads). **(D)** Quantification of **(C)** showing the outer cell wall is around 3 times as thick as inner cell walls. Cell wall thickness is measured in 129 cells from the cross sections of 4 individual Arabidopsis P_4. Scale bar, 2 µm.

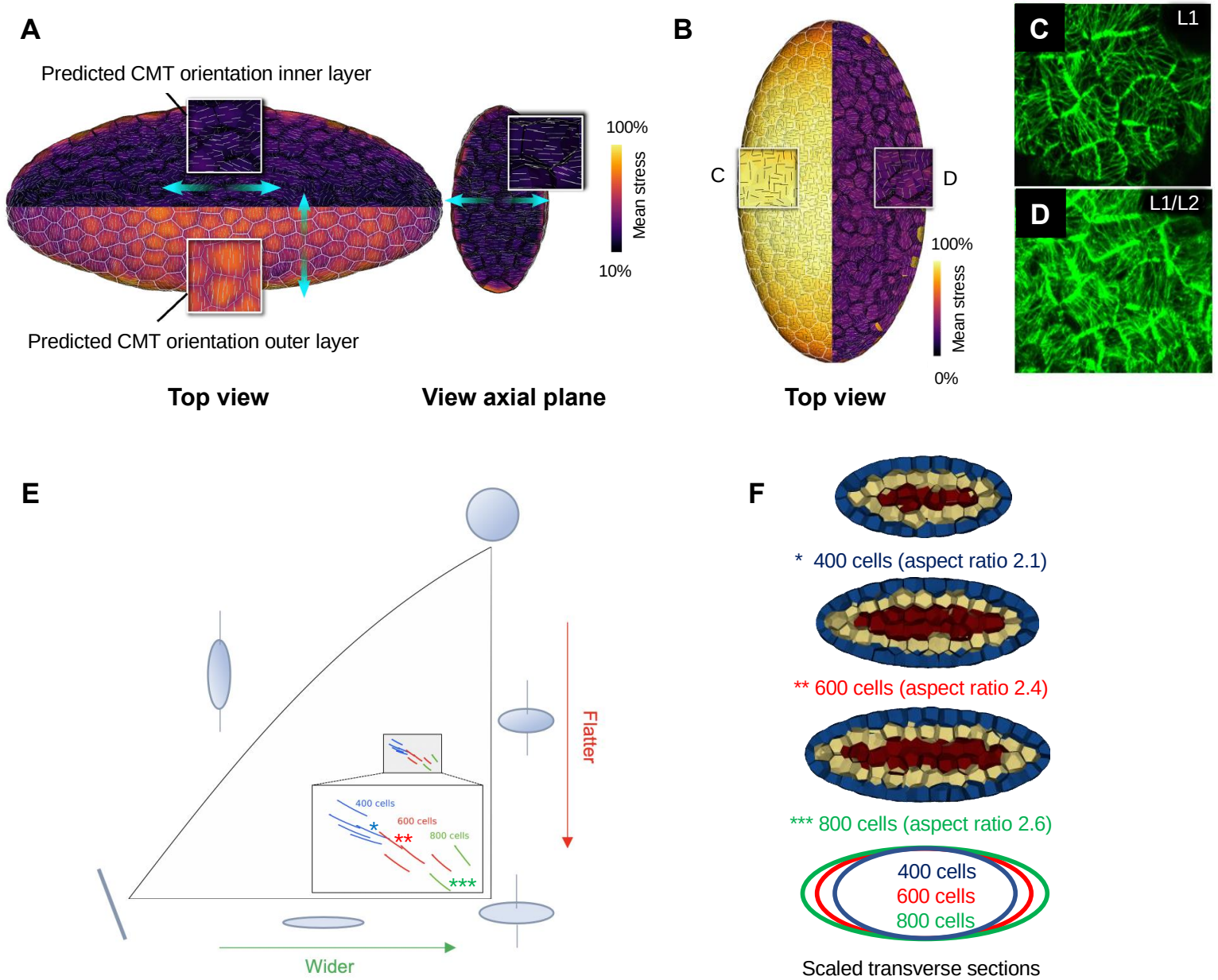
A
Predicted CMT orientation inner layer
100%
Mean stress
10%
Predicted CMT orientation outer layer
Top view
View axial plane
B
C
D
100%
Mean stress
0%
Top view
C
L1
D
L1/L2
E
Flatter
Wider
400 cells
600 cells
800 cells
*
**
***
F
* 400 cells (aspect ratio 2.1)
** 600 cells (aspect ratio 2.4)
*** 800 cells (aspect ratio 2.6)
400 cells
600 cells
800 cells
Scaled transverse sections

Figure S5. Effect of Feedback on All Walls and Simulations with Different Cell Numbers, Related to Figure 4

(**A**) When all walls in the simulation have mechanical feedback, the outer layer will mainly orient its microtubules perpendicular to the longest axis of the ellipsoid and cause the structure to lengthen. This will cause resistance of the inner cells, which will orient their microtubule along that axis. This will generate distortions in the long run. Note that in the axial plane, all simulated microtubules orient along ad-abaxial axis as also observed *in vivo*. Green arrows indicate main CMT orientations in different planes and layers. (**B**) Only the mechanical feedback on the outer periclinal walls is switched off. Under this condition, simulations predicted more or less isotropic microtubule orientations in both outer (detail in inset **C**) and inner (detail in inset **D**) cells, which are also observed *in vivo.* (**C** and **D**) Arabidopsis sepal at stage 5 showing isotropic CMTs on the outer surface (**C**) and inner (L1/L2) in-plane wall (**D).** (**E** and **F**) Simulations using structures with close anisotropies and varying numbers of cells. Feedback was introduced along all inner walls. The higher the number of cells, the larger the structure, thus mimicking the effect of cell division. Three series of simulations were performed over short periods: (i) one with a volume of 400 cells (each cell has a volume of about 125 μm^3), (ii) one with a volume of 600 cells (with the same cell volume), starting with shapes consistent with the final shapes of the simulations with 400 cells (iii) one with a volume of 800 cells. (**E**) Shape diagram showing trajectories of different shapes. The simulations clearly show a general trend towards flattening and broadening with increasing volume and increasing cell numbers thus confirming even more strongly the effect of such the feedback on flattening. Considering the total set of simulations, this would correspond to an aspect ratio (Width/Thickness) ranging from 1.8 (initial aspect ratio at 400 cells) to 2.6 (starting with shapes consistent with the final shapes of the simulations with 600 cells). (**F**) Transverse sections through endpoints of trajectories marked with * in (**E**). The scaled transverse sections are normalized for thickness to show the change in width.

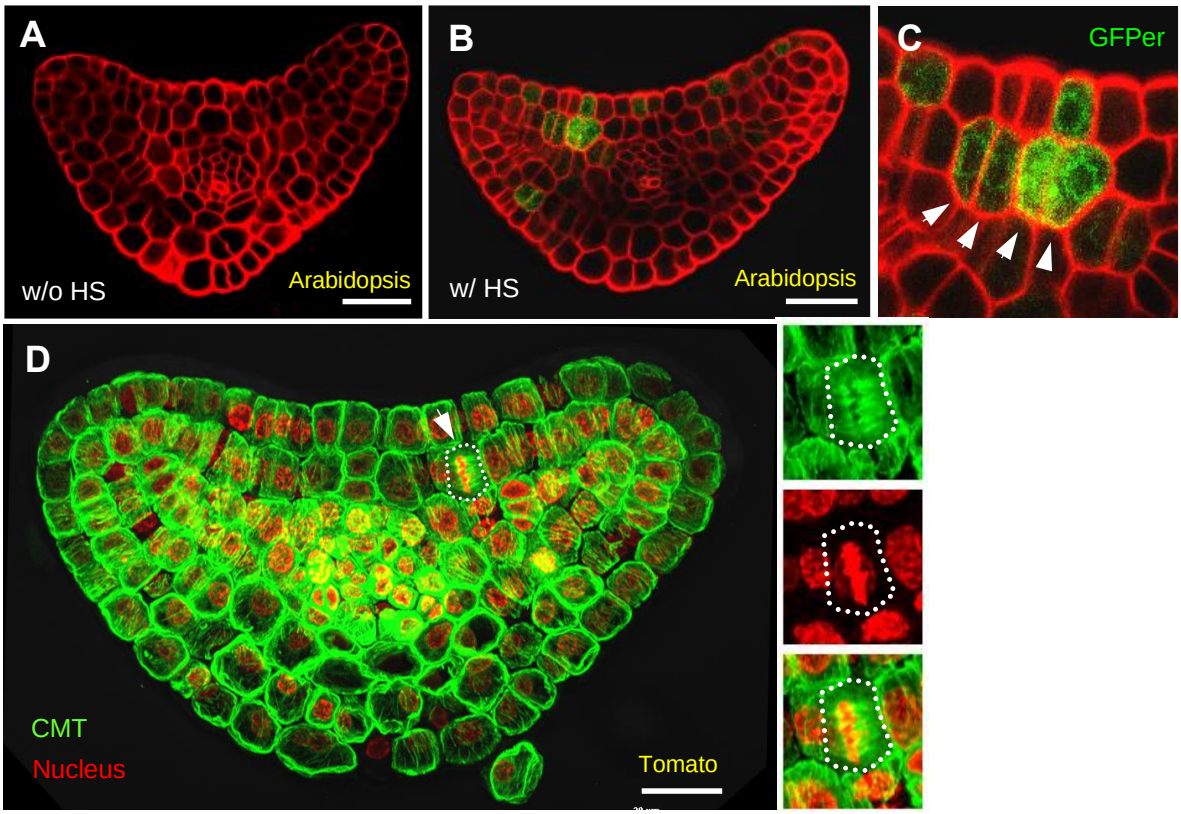
A
w/o HS
Arabidopsis
B
w/ HS
Arabidopsis
C
GFPer
D
CMT
Nucleus
Tomato
E
Tomato
F
Inner cell
Percentage of division plane
30%
25%
20%
15%
10%
5%
0%
0° 10° 20° 30° 40° 50° 60° 70° 80° 90°
G
Tomato
H
Epidermal cell
Percentage of division plane
100%
80%
60%
40%
20%
0%
0° 10° 20° 30° 40° 50° 60° 70° 80° 90°

Figure S6. Division Orientations in Inner and Epidermal Cells of Leaf Primordia, Related to Figure 6

(**A** to **C**) Cell linage tracing analysis in *Arabidopsis* leaf primordia using a heat-shock induced Cre-loxP system. No endoplasmic reticulum localized GFP signal (GFPer) is available without heat shock (w/o HS) (**A**). In leaf primordium 72 hours after heat shock (w/ HS), GFPer is observed in continuous cell files (white arrowheads) along the medio-lateral direction (**B**). (**C**) Magnification of a part of (**B**). (**D**) Immunolocalization of cortical microtubules in the cross section of a tomato P_3 with tubulin antibody (green). The chromosomes are stained by DAPI (red). Arrow indicates the cell in metaphase. Enlarged images are shown in the right panel showing the chromosomes are separated along medial-lateral direction. (**E** and **F**) The distribution of inner cell division angles (n = 153) with the medio-lateral axis labelled as blue dashed arrows (**E**) in optical cross sections of one entire tomato P_3 from the tip to the base (**F**). (**G** and **H**) The distribution of epidermal cell division angles (n = 107) with the corresponding tangent (blue dashed arrows) (**G**) in a collection of optical cross sections of one entire tomato P_3 from the tip to the base (**H**). Scale bars, 20 μm.

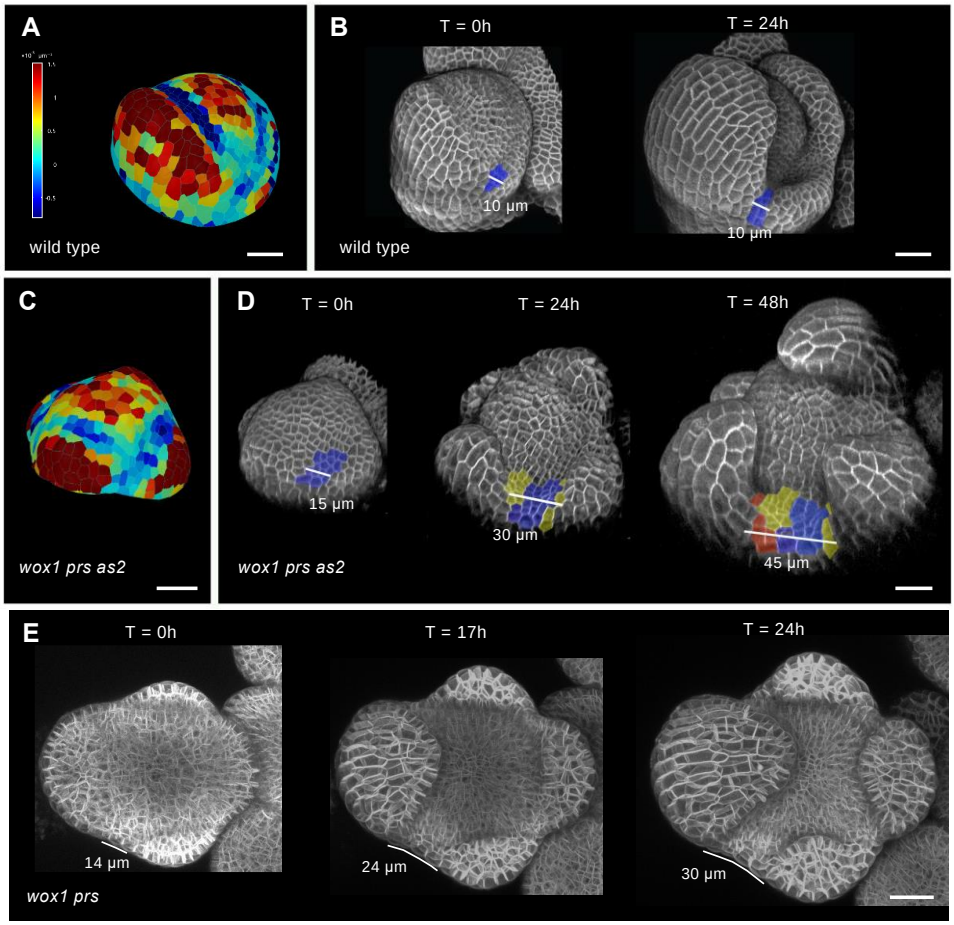

Figure S7. Boundary Formation in Wild-type, *wox1 prs as2* and *wox1 prs* Mutant Flowers, Related to Figure 7

(**A**) Segmented 3D reconstruction of a wild-type flower (expressing *p35S:GFP-Lti6b*) at 0 h, showing degree of Gaussian curvature. Blue color indicates negative curvature which is a marker for the boundary. (**B**) Confocal, 3D reconstruction showing the same flower bud at two time points. The site of negative curvature is marked blue. The width of this boundary does not change and remains about 10 µm wide. (**C**) Segmented 3D reconstruction of a *wox1 prs as2* flower (expressing *p35S:GFP-Lti6b*) at 0 h. (**D**) Development of boundary in the *wox1 prs as2* mutant at three time points. The initial zone of negative curvature is slightly broader than the wild type and then gradually increases in size (from about 15 µm to 45 µm, marked with color from blue to yellow and red). (**E**) Development of *wox1 prs* flower at three time points showing the enlarged boundaries (from about 14 µm to 30 µm, marked with white lines). Scale bars, 20 µm.